AIP | Applied Physics Letters

Ultrasensitive mid-infrared up-conversion imaging at few-photon level

Qian Zhou, Kun Huang, Haifeng Pan, E Wu, and Heping Zeng

Citation: Appl. Phys. Lett. **102**, 241110 (2013); doi: 10.1063/1.4811826
View online: http://dx.doi.org/10.1063/1.4811826
View Table of Contents: http://apl.aip.org/resource/1/APPLAB/v102/i24
Published by the American Institute of Physics.

Ultrasensitive mid-infrared up-conversion imaging at few-photon level

Qian Zhou,[1] Kun Huang,[1] Haifeng Pan,[1] E Wu,[1,a)] and Heping Zeng[1,2,b)]
[1]*State Key Laboratory of Precision Spectroscopy, East China Normal University, Shanghai 200062, China*
[2]*Shanghai Key Laboratory of Modern Optical System, Engineering Research Center of Optical Instrument and System, Ministry of Education, School of Optical-Electrical and Computer Engineering, University of Shanghai for Science and Technology, Shanghai 200093, China*

(Received 21 November 2012; accepted 9 June 2013; published online 20 June 2013)

We demonstrated few-photon-level mid-infrared imaging at 3.39 μm by efficient frequency up-conversion. The quantum frequency up-conversion efficiency of mid-infrared photons was high to 32.9%, while mid-infrared images were up-converted with the quantum efficiency of 12.5%. The mid-infrared imaging sensitivity was improved by counting the frequency up-conversion photons temporally confined within the time-window of the pump pulse. The frequency up-conversion system induced a background noise of 1.1×10^3 counts per second. © *2013 AIP Publishing LLC*. [http://dx.doi.org/10.1063/1.4811826]

Recently, with development of laser techniques, the mid-infrared sources can be readily attained by quantum cascade lasers, semiconductor lasers, and four-wave mixing in filaments.[1–4] Mid-infrared lasers are widely used in revealing molecular rovibrational transitions, detecting spectral fingerprints of carbon-hydrogen bonds, monitoring atmospheric trace molecules, sensing various types of environmental gases, and even analyzing exhaled human breath for medical diagnostics.[5–7] However, all the mid-infrared applications urgently call for dramatic improvement of mid-infrared detection and imaging systems with high-sensitivity and low dark noise. So far, the mid-infrared detection techniques have lagged far behind the rapid development of the mid-infrared sources. Though many efforts have been focused on developing semiconductor detectors[8] such as HgCdTe, InSb, GaSb, and PbSe, most of the mid-infrared detectors have quite low sensitivities and large dark noise inherent from the low energy band-gap semiconductors used for photodetection. Mid-infrared imaging devices encounter even more severe difficulties of quite large dark noise. For instance, the widely used InSb-based mid-infrared cameras,[9] even cryogenically cooled, have the dark noise at least ten orders of magnitude above the single-photon photo-current, prohibitive for any imaging at quantum level, while presently available HgCdTe detectors[10] offer relatively high mid-infrared sensitivity that are ideal for low-throughput analysis as high sampling rates are required. Various HgCdTe photodiode array detectors are invented for the mid-infrared imaging applications.[11] The corresponding severe dark currents need to reduce billion times to reach the mid-infrared quantum detection regime. It is highly desired for all the mid-infrared applications to improve the detection and imaging sensitivity, and some ultra-high sensitivity applications even require mid-infrared photon detection and imaging techniques, stimulating a burgeoning area of mid-infrared quantum photonics.

On the other hand, mid-infrared photons could be up-converted into visible or near-infrared ones via nonlinear frequency up-conversion, exhibiting the potential for ultrahigh-sensitivity detection of mid-infrared photons. Such frequency up-conversion techniques were proposed as early as 1960s, but continuous experimental explorations in past 50 years failed in reaching sufficiently high up-conversion efficiencies. Nearly unitary up-conversion efficiency typically requires a sufficiently strong pump in a quadratic transparent crystal with a large optical nonlinearity, which nevertheless induces quite large parametric scattering noises.[12] Frequency up-conversion of mid-infrared images was demonstrated to be of no practical meanings under weak continuous-wave pumping. A breakthrough in improving the frequency up-conversion efficiency was made in 2012 with a continuous-wave intracavity pump scheme, based on which a quantum efficiency of 20% was achieved for up-conversion of mid-infrared photons at 3–4 μm.[13] Actually, such an intracavity pump scheme was previously demonstrated to support an efficiency of 96% in up-converting single photons at the telecom wavelength.[14] As the frequency up-conversion was controlled to reach nearly unitary conversion efficiency, quantum features of the mid-infrared photons could be completely transferred to the up-converted photons.[15] This is anticipated to benefit mid-infrared imaging at few-photon level. By using electron multiplying silicon charged coupled devices (EMCCDs) to directly record the up-converted photons in the visible or near-infrared region, the efficient quantum up-conversion detection could be extended to ultra-sensitive mid-infrared imaging at few-photon level with high quantum efficiency and good spatial resolution.

In this letter, we present the experimental demonstration of few-photon-level mid-infrared imaging at 3.39 μm based on pulse-gated frequency up-conversion. As benefited from the intense peak power of the pulsed pump, quite efficient frequency up-conversion could be achieved with a modest average pump power.[12,16,17] Mid-infrared photons at 3.39 μm were up-converted with a conversion efficiency of 32.9%, while mid-infrared images were frequency up-converted with a conversion efficiency of 12.5%. Under such an efficient frequency up-conversion, the mid-infrared images were conveniently detected by a high-performance

a)Electronic address: ewu@phy.ecnu.edu.cn.
b)Electronic address: hpzeng@phy.ecnu.edu.cn.

EMCCD. The pulsed pump equivalently functioned as an effective gate to reduce the background noise. As a result, the sensitivity of the up-conversion imaging was improved by counting the frequency up-conversion photons temporally confined within the time-window of the pumping pulse. The background noise was measured to be 1.1×10^3 counts per second (cps).

The frequency up-conversion detection scheme is illustrated in Fig. 1. The experimental setup consisted of pump and signal sources, frequency up-conversion, and imaging system. The mid-infrared signal source was provided by a He-Ne laser operated at 3.39 μm with a bandwidth less than 0.3 nm (PLASMA GNIK-3-1A). The signal light illuminated onto the transmission mask of three equally spaced vertical slits to form the object beam, and the size of the squared image was 1.5 mm. The mid-infrared imaging photons from the He-Ne laser were spectrally up-converted to near-infrared via sum frequency generation (SFG) in an MgO-doped periodically poled lithium niobate (PPLN) crystal. MgO-doped PPLN was used mostly because of its large nonlinear optical coefficient and low photo-refraction influence. The periodically poled structure supported a relatively long quasi-phase-matching distance. We used a 50-mm-long MgO:PPLN crystal in our experiment. For the mid-infrared up-conversion, we need to concern the working temperature for the purpose to lessen the thermal emission. The up-conversion was performed in an MgO:PPLN crystal of appropriate poling period so that quasi-phase matching condition could be reached slightly above room temperature, at which the MgO:PPLN crystal emitted negligible thermal radiation in the infrared wavelength region of interest. With a poling period of 22.35 μm, the MgO:PPLN working temperature was well-controlled at 28.7 °C with a fluctuation less than 0.1 °C.

The pump source was a passively mode-locked ytterbium-doped fiber laser with a repetition rate of 17.2 MHz. A 3-nm band-pass filter centered at 1050 nm was used in the laser cavity to get a pump source of narrow output spectrum. In order to satisfy the quasi-phase-matching bandwidth of the MgO:PPLN crystal (0.3 nm), a 0.3-nm bandwidth fiber Bragg grating (FBG) for 1050 nm was employed at the output of the ytterbium-doped fiber laser. The FBG-filtered laser output with 0.3-nm bandwidth was then amplified by two ytterbium-doped fiber amplifiers as the pump source. The maximum output power reached 28.8 mW and the pulse duration was measured to be 5.3 ps. The corresponding peak power reached 300 W. A long-pass filter cutting off at 1000 nm was used at the output of the pump beam to suppress the stray light background noise from the amplifiers. Two Glan prisms were used in front of the two beams, respectively, to select the vertical polarization to meet the requirement of quasi-phase-matching in the MgO:PPLN crystal. The object and pump beams were separately collimated and combined by a dichroic mirror, and then focused to optimize their spatial overlapping at the center of the precisely aligned MgO:PPLN crystal. The object field was transformed by a lens L1 (f = 100 mm) to the Fourier plane of the 4-f imaging system, which was located at the center of the 50-mm-long MgO:PPLN crystal. The up-converted image was collected and collimated by a lens L3 (f = 300 mm), and then directly detected by the EMCCD located at the image plane.

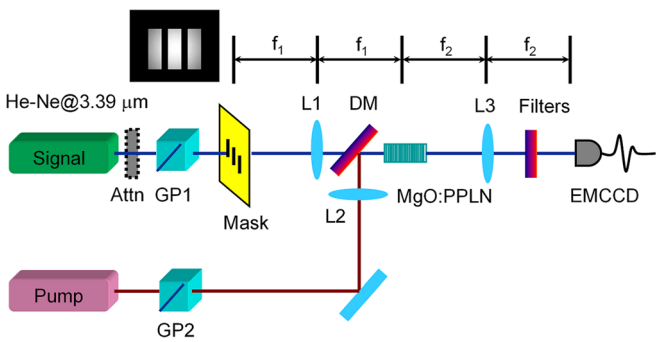

FIG. 1. Experimental setup of mid-infrared frequency up-conversion imaging system. Attn, attenuator; GP1 and GP2, Glan prism; DM, dichroic mirror; L1, L2, L3, lens; MgO:PPLN, MgO-doped periodically poled lithium niobate crystal; EMCCD, silicon electron multiplying charged coupled device.

The mid-infrared object beam was up-converted through SFG to generate the near-infrared image at 802 nm. At first, we removed the mask and used a Si-avalanche photodiode (Si-APD) single-photon detector to evaluate the up-conversion efficiency. Before injecting on the Si-APD detector, a filtering system, consisting of two high-reflection mirrors, a band-pass filter, and a short-pass filter, was used to cut down the background noise. Due to dispersion in the lithium niobate crystal, walk-off between the signal and pump should be considered in the 50-mm-long MgO:PPLN crystal. The walk-off parameter is given by

$$d_{12} = \beta_1(\lambda_1) - \beta_1(\lambda_2), \tag{1}$$

where λ_1 and λ_2 are the signal and pump wavelengths, respectively, and $\beta_1 = \frac{1}{c}\left(n + w\frac{dn}{dw}\right)$, with n as a function of wavelength being the refractive index of the lithium niobate crystal. Then we got the walk-off parameter $d_{12} = 247$ ps/m, and the walk-off time $t_0 = 12.4$ ps. And the walk-off length $L_W = T_0/|d_{12}|$ was calculated to be 21.5 mm, where $T_0 = 5.3$ ps was the pulse duration of the pump pulses. As thus, the temporal overlap between the signal and pump sources could be defined as

$$t = \sqrt{T_0^2 + t_0^2}, \tag{2}$$

which was calculated to be 13.5 ps. As the signal was in the continuous-wave mode while the pump pulses came from the mode-locked laser, the duty cycle ratio of the pump source was 2.3×10^{-4}. As the incident power of the signal source was 64.4 nW, the total energy of the signal photons which was enveloped by each pump pulse was 3.7×10^{-6} nJ, corresponding to 6.3×10^4 photons. A density attenuation of 44.4 dB was inserted after the He-Ne laser, and the signal at 3.39 μm was attenuated to few-photon level about 2.3 photons per pulse for the mid-infrared imaging. Then the up-converted photons with unitary conversion efficiency were calculated to be 3.9×10^7 cps. The photon counting of the Si-APD was recorded as a function of the average pump power. The maximum detected photon counting of 4.1×10^6 cps was achieved at the pump power of 28.8 mW. Therefore,

the maximum detection efficiency of 10.5% was deduced from 4.1×10^6 cps/3.9×10^7 cps. Considering that the transmittance of the whole filtering system was about 57.9% and the quantum efficiency of the Si-APD was about 55%, the corresponding conversion efficiency was inferred to be 32.9%.

The sum-frequency generation technique is characterized by the up-conversion efficiency η as

$$\eta = \sin^2[\pi\sqrt{P_p}/2\sqrt{P_c}], \tag{3}$$

where P_p is the incident pump power to the nonlinear crystal and P_c is the pump power required to achieve unity conversion efficiency. The experimental conversion efficiency (the closed red circles) as a function of the pump power and the corresponding theoretical fitting (the black line) according to Eq. (3) are shown in Fig. 2. According to the theoretical fitting, we obtained $P_c \approx 200$ mW.

The background counts recorded as a function of the pump power without mid-infrared photon injection are also shown in the inset of Fig. 2. In this setup, the largest total background noise was about 1.1×10^3 cps including the Si-APD dark counts of ~300 cps, meaning that the noise probability per pulse was about 6×10^{-5}, which was deduced from 1.1×10^3 cps/17.2 MHz. The total background noise was one of the most important factors which determined the experimental sensitivity. Background noises consisted in all counts generated from external photons other than the signal photons in frequency up-conversion system, including leakage of laser light, dark counts of the Si-APD, and up-conversion of thermal radiation.[18] In the mid-infrared imaging detection system, as the pump beam was spatially Gaussian-shaped, the noise from the up-converted blackbody radiation was also in Gaussian profile. As thermal light from blackbody radiation obeys the Bose–Einstein probability distribution,[19] by assuming that only one spatial mode is up-converted, the background noise count rate caused by blackbody radiation can be expressed as

$$\langle n_{BG}\rangle = \eta_{tot}\int_{-\infty}^{\infty}\frac{T(v)dv}{\exp(hv/kT)-1} \approx \frac{\eta_{tot}\Delta v}{\exp(hv_0/kT)-1}, \tag{4}$$

where η_{tot} is the total quantum efficiency of the system defined by the probability that an incoming photon generates a counting event, $T(v)$ is the overall normalized transfer function of the optical components, $[\exp(hv/kT)-1]^{-1}$ is the mean number of photons per mode and $\Delta\nu/[\exp(hv_0/kT)-1]$ is the mean blackbody radiation photon rate. For the sake of simplicity, we approximate $T(v)$ as a delta function, the full spectral integration thus covers Δv bandwidth centered at $v_0 = c/\lambda_{signal}$. According to Eq. (4), the blackbody background noise increases with the overall efficiency. Then the total noise count rate can be given by $\langle n_{tot}\rangle = \langle n_{BG}\rangle + \langle n_{DC}\rangle$, where $\langle n_{DC}\rangle$ is the background noise count rate caused by APD's dark counts, which is about 300 cps in our experiment. And $\langle n_{BG}\rangle$ is dependent on the detection efficiency. Therefore, the dominative factor on the total noise is the blackbody background noise when the conversion efficiency increases. In the experiment, the blackbody background noise was mainly caused by the thermal radiation in the frequency up-conversion crystal. At the operating temperature of 28.7 °C, the MgO:PPLN crystal emitted almost no observable thermal radiation in the mid-infrared region around 3.39 μm.[20] And very few blackbody background photons were temporally confined within the time-window of the pumping pulse and frequency-up-converted to the visible regime, leading to the noise counts in the detection.

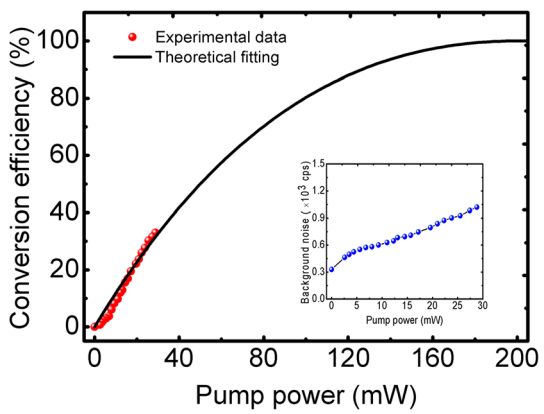

FIG. 2. Conversion efficiency as a function of pump power. Inset: Background noise as a function of the pump power.

Combining frequency up-conversion system and advanced silicon EMCCD,[13] mid-infrared image at few-photon level could be obtained with quite high sensitivity and good spatial resolution. Then we inserted a mask in the input infrared beam to check its influence on the mid-infrared single-photon frequency-up-conversion. We first verified the conversion efficiency by focusing all the up-converted photons to the single-photon detector. With the signal light illuminating the mask of three equally spaced vertical slits, the detection efficiency reached 7.7%. The corresponding conversion efficiency was inferred to be 12.5%. Without the mask, the conversion efficiency reached up to 32.9% as the Gaussian-shaped signal beam was more concentrated at the Fourier plane without the effect of Fraunhofer diffraction. The distribution of the laser field at the Fourier plane is displayed in Fig. 3(a), while Fig. 3(b) shows the filtered Fourier transformation patterns by the pump beam. The pump beam at 1050 nm had a Gaussian profile and it worked as a Gaussian spatial filter in our system. Thus, the low spatial frequency components located at the center of the focused pump beam could be more efficiently up-converted than the high spatial frequency components. According to the simulation, the ratio of signal beam power after and before the spatial filtering induced by the pump is 0.59.

After that, we replaced the single-photon detector by the EMCCD camera to catch the image. The signal at 3.39 μm was intentionally attenuated to few-photon level to test the mid-infrared imaging sensitivity. The up-converted images were registered by using an EMCCD (iXon3 897, Andor) thermoelectrically cooled to −85 °C to lower the dark noise. The EMCCD was a silicon-based semiconductor chip of 512×512 pixels. Each pixel covered a size of 16×16 μm^2, suitable for high spatial resolution imaging.[21] For the object beam, we set the integration time of 2 s, and accumulated once for each acquisition. Figure 3(c) shows the simulated up-conversion images, while the up-converted images at

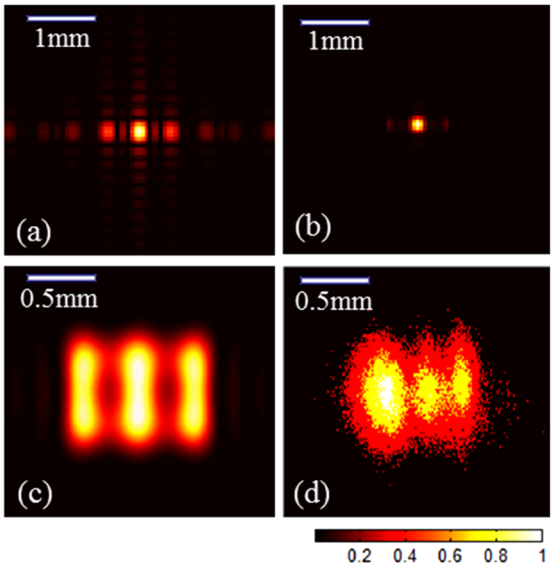

FIG. 3. Distribution of electric field of the signal beam at the Fourier plane (a), the filtered Fourier transformation pattern by the pump beam (b), theoretical simulation of up-converted image with strong object beam light (c), and experimentally obtained up-converted image at few-photon level (d).

few-photon level are shown in Fig. 3(d). The images could be seen clearly but with blurred edges. The image distortion was ascribed to the point spread function effect in the up-conversion imaging system.[21,22]

In conclusion, we demonstrated few-photon-level mid-infrared imaging at 3.39 μm by efficient frequency up-conversion system with low background noise. Benefited from pulsed pump at 1050 nm, high conversion efficiency was achieved with modest pump power. The mid-infrared photons of up-converted images were captured by the silicon EMCCD with high sensitivity and good spatial resolution. The compact fiber laser pumped up-conversion imaging system may offer promising applications that require ultra-sensitive mid-infrared imaging such as gas analysis and medical diagnostics. Furthermore, with coincidence frequency up-conversion based on the synchronized signal and pump sources,[23] efficient mid-infrared up-conversion imaging was achieved, which may stimulate interesting explorations on quantum information processing with mid-infrared photons.

This work was funded in part by National Natural Science Fund of China (10990101, 60907043, and 91021014), International Cooperation Projects from Ministry of Science and Technology (2010DFA04410), Key project sponsored by the National Education Ministry of China (109069), Research Fund for the Doctoral Program of Higher Education of China (20090076120024), and the Program of Introducing Talents of Discipline to Universities (B12024).

[1]T. Fuji and T. Suzuki, Opt. Lett. **32**, 3330 (2007).
[2]M. Ebrahim-Zadeh and I. Sorokina, *Mid-Infrared Coherent Sources and Applications* (Springer, Dordrecht, 2008).
[3]M. Murray, T. Fernandez, B. Richards, G. Jose, and A. Jha, Appl. Phys. Lett. **101**, 141107 (2012).
[4]A. Al-kadry and M. Rochette, J. Opt. Soc. Am. B **29**, 1347 (2012).
[5]R. Curl and F. Tittel, Annu. Rep. Prog. Chem., Sect. C: Phys. Chem. **98**, 217 (2002).
[6]P. Werlea, F. Slemra, K. Maurera, R. Kormannb, R. Mücke, and B. Jänkerd, Opt. Lasers Eng. **37**, 101 (2002).
[7]J. Houghton, Rep. Prog. Phys. **68**, 1343 (2005).
[8]B. Klein, E. Plis, M. Kutty, N. Gautam, A. Albrecht, S. Myers, and S. Krishna, J. Phys. D: Appl. Phys. **44**, 075102 (2011).
[9]L. Qin, Z. Hou, Y. Wu, F. Tan, and F. He, Laser Infrared **39**, 155 (2009). http://magazine.laser-infrared.com/ch/reader/view_abstract.aspx?flag=1&file_no=M390210&journal_id=jgyhw.
[10]W. Hu, X. Chen, F. Yin, Z. Quan, Z. Ye, X. Hu, Z. Li, and W. Lu, J. Appl. Phys. **105**, 104502 (2009).
[11]P. Hamm, S. Wiemann, M. Zurek, and W. Zinth, Opt. Lett. **19**, 1642 (1994).
[12]K. Huang, X. Gu, H. Pan, E Wu, and H. Zeng, IEEE J. Sel. Top. Quantum Electron. **18**, 562 (2011).
[13]J. Dam, P. Tidemand-Lichtenberg, and C. Pedersen, Nat. Photonics **6**, 788 (2012).
[14]H. Pan, H. Dong, and H. Zeng, Appl. Phys. Lett. **89**, 191108 (2006).
[15]J. Huang and P. Kumar, Phys. Rev. Lett. **68**, 2153 (1992).
[16]H. Dong, H. Pan, Y. Li, E. Wu, and H. Zeng, Appl. Phys. Lett. **93**, 071101 (2008).
[17]X. Gu, K. Huang, Y. Li, H. Pan, E. Wu, and H. Zeng, Appl. Phys. Lett. **96**, 131111 (2010).
[18]S. Guha and J. Falk, J. Appl. Phys. **53**, 2854 (1982).
[19]B. Saleh and M. Teich, *Fundamentals of Photonics* (Wiley, New York, 1991).
[20]J. Schwesyg, C. Phillips, K. Ioakeimidi, M. Kajiyama, M. Falk, D. Jundt, K. Buse, and M. Fejer, Opt. Lett. **35**, 1070 (2010).
[21]K. Huang, X. Gu, H. Pan, E. Wu, and H. Zeng, Appl. Phys. Lett. **100**, 151102 (2012).
[22]C. Pedersen, E. Karamehmedović, J. Dam, and P. Lichtenberg, Opt. Express **17**, 20885 (2009).
[23]G. Temporão, S. Tanzilli, H. Zbinden, and N. Gisin, Opt. Lett. **31**, 1094 (2006).